How to extract distributed circuit parameters from the scattering parameters of a transmission line

Nathan D. Orloff[1], Nina Popovic[2], Jasper A. Drisko[1], Angela Stelson[1], Charles A. E. Little[1,2], James C. Booth[1], Jordi Mateu[3], and Christian J. Long[1]

[1]National Institute of Standards and Technology, Boulder, CO, [2]University of Colorado, Boulder, CO, [3]Universitat Politecnica de Catalunya, Catalunya, Spain

Abstract — **Distributed circuit parameters parameterize the transmission and reflection off a given transmission line in terms of a distributed resistance, inductance, capacitance, and conductance, which are per-unit-length, frequency-dependent quantities. While there are analytical models for extracting the distributed circuit parameters, these models are discontinuous as a function of frequency when the argument approaches a branch cut. Here, we develop a nonlinear least-square regression algorithm that accurately extracts the distributed circuit parameters. Compared to existing approaches and finite element models, our algorithm successfully extracts the distributed circuit parameters as a function of frequency, all while being less sensitive to these phase conditions. Such an algorithm is useful for understanding how to deembed transmission lines, and how to extract electrical properties of the materials used in a circuit.**

Index Terms — **transmission line, fitting, distributed circuit parameters, S-parameters.**

I. INTRODUCTION

Understanding how voltages and currents propagate in a transmission line has been important to electrical engineers since the invention of the first working telegraph in 1816 by Francis Rolands [1]. Indeed, some of the greatest pioneers in electricity and magnetism got their start on this very topic. Chief among them is Oliver Heaviside, who was the first to write down what we commonly refer to as the telegrapher's equations [2]. The Telegrapher's equations describe how a voltage and current change as a function of time as they propagate down a transmission line. At their conception, these equations allowed electrical engineers to predict how far their signals could propagate and account for distortion.

Since then, Telegrapher's equations have become an essential part of every electrical engineer's toolbox. We use them to model the magnitude and phase of a voltage and current at a given position and time, whether that be in an integrated circuit or coaxial cable. In fact, there are very good analytical models of the distributed circuit parameters in the literature, with several outstanding examples for coplanar waveguide (CPW) transmission lines [3], [4]. More generally, we can measure the scattering (S-) parameters of a transmission line, correct them, and then use analytical models to extract the distributed circuit parameters [5]. This analytical approach is useful when the exact geometry of the transmission line is unknown, or when there is no analytical model that describes this specific type of transmission line. The problem with this approach lies in the phase of the reflection and the transmission as a function of frequency. At a high enough frequency, these phases produce a branch cut in the argument used to compute the propagation constant, which results in a large discontinuity in the extracted distributed circuit parameters.

Inspired by previous work, we have developed a nonlinear least-squares algorithm to mitigate this problem, and permit the extraction of the distributed circuit parameters over the full frequency regime. Our approach starts with corrected S-parameters of a transmission line. We then computed estimates for the distributed circuit parameters, and scale them such that they all varied with the same frequency dependence and had an order of magnitude close to one. We then passed the estimates to the nonlinear least-squares optimization algorithm, computed the difference between the model and the data, and minimized the difference. The key idea was to scale the distributed circuit parameters, which improved how we used trust-region-reflective [6] and Levenberg-Marquardt [7], [8] optimization. There are some potential trade-offs to our algorithm. If the distributed circuit parameters are negative as a function of frequency, then our algorithm may need to be modified to work.

In this paper, we demonstrate that the distributed circuit parameters can be fit with a nonlinear least-squares algorithm, which considers the relative scaling of the fit parameters to minimize the sensitivity of the fit to phase of the S-parameters. We describe our algorithm step-by-step and explain the reasoning behind each step. We validate our algorithm with coplanar waveguide transmission lines on fused silica substrate, which were corrected with an optimized multiline thru-reflect-line (TRL) calibration algorithm. After applying our algorithm, we compare the distributed circuit parameters extracted with analytical expressions and our algorithm, which we contrast to finite element simulations of the same transmission lines. Taken together, this paper provides a detailed description of an algorithm to extract the distributed circuit parameters of a transmission line as a function of frequency that is more robust against the phase uncertainties than analytical models.

II. THEORY

For a lossy transmission line, we parameterize the distributed circuit in terms of a resistance (R), inductance (L), capacitance (C), and conductance (G) per unit length.
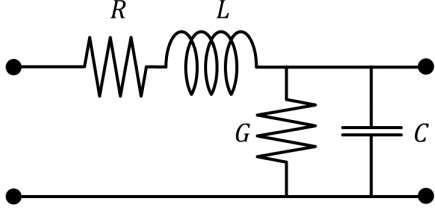
Fig. 1. The distributed circuit for a transmission line modeled by a resistance (R), inductance (L), capacitance (C) and conductance (G) per unit length.

In the most general sense, R, L, C and G depend on frequency (Fig. 1). Applying Kirchhoff's point and loop rules to Fig. 1, we obtain the Telegrapher's equations,

$$\frac{\partial}{\partial x}\tilde{V}(x) = -L\frac{\partial}{\partial t}\tilde{I}(x) - R \cdot \tilde{I}(x) \text{ and}$$
$$\frac{\partial}{\partial x}\tilde{I}(x) = -C\frac{\partial}{\partial t}\tilde{V}(x) - G \cdot \tilde{V}(x). \tag{1}$$

Next, we assume a sinusoidal time dependence,

$$I(x,t) = \tilde{I}(x) = I(x)e^{i\omega t} \text{ and}$$
$$V(x,t) = \tilde{V}(x) = V(x)e^{i\omega t}. \tag{2}$$

Then, we insert (2) into (1), and solve the wave equation to define the propagation constant,

$$\gamma = \sqrt{(R + i\omega L)}\sqrt{(G + i\omega C)}, \tag{3}$$

and the characteristic impedance,

$$Z = \frac{\sqrt{(R + i\omega L)}}{\sqrt{(G + i\omega C)}}. \tag{4}$$

A. Eiensentadt's analytical model for transmission lines

Now that we understand where the distributed circuit parameters come from, we can use them to develop analytical models of a transmission line. In [5], Eisenstadt and Eo developed their analytical expressions for γ and Z from ABCD matrices. In general, ABCD-parameters are convenient for modeling both lumped element and distributed circuits, as well as for cascading elements together [9]. A general ABCD matrix is given by,

$$M = \begin{pmatrix} A & B \\ C & D \end{pmatrix}. \tag{5}$$

ABCD-parameters are also intuitive, because they relate physical currents and voltages in a two-port network. We can convert S-parameters to ABCD-parameters following the expressions in Refs. [5] and [9].

For a uniform two-port transmission line of length ℓ corrected to a characteristic impedance Z_r, the ABCD-parameters are given by,

$$M = \begin{pmatrix} cosh(\gamma\ell) & Z_r \cdot sinh(\gamma\ell) \\ \frac{1}{Z_r} \cdot sinh(\gamma\ell) & cosh(\gamma\ell) \end{pmatrix} \tag{6}$$

We take (6), combining terms and geometrical identities, to derive an argument involving the propagation constant (γ) and length of the transmission line (ℓ),

$$e^{-\gamma\ell} = cosh(\gamma\ell) + sinh(\gamma\ell)$$
$$= \frac{A+D}{2} + \sqrt{B \cdot C} \tag{7}$$

Eisenstadt and Eo [5] took (7) one step further and solved for γ and Z in terms of the corrected S-parameters. We use this analytical model for comparison here. For completeness, we reproduce these expressions here,

$$\gamma = -\frac{1}{\ell}\ln\left[\left\{\frac{1 - S_{11}^2 + S_{21}^2}{2S_{21}} \pm K\right\}^{-1}\right]$$
$$K = \left\{\frac{(S_{11}^2 - S_{21}^2 + 1)^2 - (2S_{11})^2}{(2S_{21})^2}\right\}^{\frac{1}{2}} \tag{8}$$

and the characteristic impedance,

$$Z^2 = Z_r^2 \frac{(1 + S_{11})^2 - S_{21}^2}{(1 - S_{11})^2 - S_{21}^2}. \tag{9}$$

The problem with (8) and (9) are the potential sign ambiguities that arise when the phase of the argument in (8) go through π or $-\pi$. As in Ref. [5], we compute R, L, C and G,

$$R = \Re(\gamma \cdot Z) \tag{10}$$
$$L = \Im(\gamma \cdot Z)/\omega \tag{11}$$
$$C = \Im\left(\frac{\gamma}{Z}\right)/\omega, \text{ and} \tag{12}$$
$$G = \Re\left(\frac{\gamma}{Z}\right). \tag{13}$$

B. Our analytical model for transmission lines

Instead of the Eisenstadt and Eo [5] model, we used the T-matrix form of a transmission line, because the T-matrix formalism does not require a defined reference impedance. In this case, the model for the T-matrix of a transmission line in a 50 Ω reference impedance is,

$$T = Q_Z^{50} \begin{pmatrix} e^{-\gamma\ell} & 0 \\ 0 & e^{\gamma\ell} \end{pmatrix} Q_{50}^Z, \tag{14}$$

where the impedance transformer is given by,

$$Q_{Z_m}^{Z_n} = \frac{1}{2\sqrt{Z_n \cdot Z_m}}\begin{pmatrix} Z_m + Z_n & Z_m - Z_n \\ Z_m - Z_n & Z_m + Z_n \end{pmatrix}. \tag{15}$$

We have used this model with great success in the past; see, for example, Refs. [10]–[14].

III. FABRICATION

We fabricated the CPW devices on a 500 μm thick, 7.62 cm diameter fused silica (quartz) wafer. We chose quartz, because it has low electrical conductivity and isotropic permittivity [15].

The electrode layer consisted of a 5 nm Ti adhesion layer followed by 500 nm of Au that we deposited by electron beam evaporation. The CPWs on the calibration chip had a nominal characteristic impedance of ~50 Ω with 20 μm-wide center conductors, 2 μm-wide gaps, and 200 μm-wide ground planes (Fig. 2). The devices on the calibration chip had contact pads for on-wafer probe measurements. The pads were reinforced with ~115 nm of palladium, which was used for the contact pads due to its low evaporation temperature, minimal oxidation, and hardness [14].
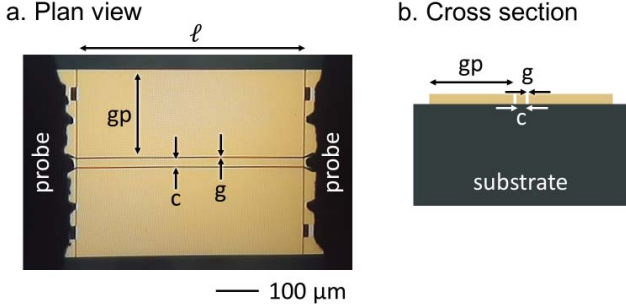

Fig. 2. (a) A plan view of a coplanar waveguide transmission line with measurement probes. (b) The cross section of the coplanar waveguide transmission line. In both (a) and (b), the center conductor is labeled c, the gap is labeled g, and the ground plane is labeled gp. The center conductor was nominally 20 μm wide, the gap was nominally 2 μm wide, and the ground plane was nominally 200 μm wide. The coplanar waveguide transmission line has a length ℓ.

IV. STEP-BY-STEP ALGORITHM

1. Measure and then correct S-parameters of uncorrected transmission line.
2. Estimate initial guess of the distributed circuit parameters, with either finite-element simulations, or analytical models.
3. Scale the estimates for the initial guess of the distributed circuit parameters.
4. Impose physical bounds. Optional: Impose recursion.
5. Apply nonlinear least-squares routine:
   a. Rescale estimates for the distributed circuit parameters.
   b. Compute the T-matrix model for the transmission line.
   c. Compute and return the error function.
6. Return the optimized distributed circuit parameters.

V. SCALING

The key idea in this paper and the real contribution to the literature is the realization that the distributed circuit parameters can be scaled to roughly the same order of magnitude. This scaling is a critical part of optimally leveraging the strengths of the trust-region-reflective [6] and Levenberg-Marquardt [7], [8] optimization.

On close examination of [16], Marks and Williams identified some important relationships; namely, R, L, C and G are directly related to Maxwell's equations through the material properties used to make the transmission line. For simplicity, the distributed circuit parameters are related to physical material properties and associated integrals through,

$$R \propto \omega(\mu_i) \text{ and/or } \sigma \cdot \sqrt{\omega}, \quad (16)$$
$$L \propto \mu_r, \quad (17)$$
$$C \propto \epsilon_r, \text{ and} \quad (18)$$
$$G \propto \omega \epsilon_i. \quad (19)$$

Here, the complex permittivity of the transmission line is given by $\epsilon = \epsilon_r - i\epsilon_i$, the complex permeability is $\mu = \mu_r - i\mu_i$, and the conductivity of the conductors is σ.

From these relationships, (14)-(15), we know that G/ω has the same units as C, and that (14)-(15) are proportional to the complex permittivity. Typically, our CPWs have a capacitance around 1 pF/cm. Furthermore, we know that changes in both the real and imaginary part necessarily have the same order of magnitude due to the Kramers-Kronig relations [17]. We can understand R and L by considering a nonmagnetic transmission line where $\mu_r = 1$ and $\mu_i = 0$. In this case, this assumption reduces (12) to a geometrical constant multiplied by the conductivity of the conductors and the square root of frequency. Thus, we can decrease the frequency dependence $R/(\sqrt{\omega})$ must have roughly the same order of magnitude as L. The last step in the scaling is to take $\log_{10}(R, L, C, \text{and } G)$, take the mean of this value, and then divide its order of magnitude to scale the distributed circuit parameters to values around one. This last step is essential for leveraging conventional optimization routines.

VI. MEASUREMENT AND CALIBRATION

We measured the S-parameters with a vector network analyzer (VNA), contacting each structure with on-wafer probes. We moved the probes to measure each device. For these measurements, we measured 512 frequency points from 70 kHz to 110 GHz with -20 dBm signals that had an intermediate frequency bandwidth of 50 Hz. We performed all measurements on a temperature controlled probe station.

C. On-wafer calibration

Our approach relies on an on-wafer calibration, where the calibration used S-parameters measurements of known artifacts on the calibration chip. We also measured the switch terms, and corrected for switch terms [18].

To perform the on-wafer calibration, we measured the S-parameters of seven different-length CPWs with $\ell = (0.420, 1.000, 1.735, 3.135, 4.595, 7.615, 9.970)$ mm, a series resistor, a series capacitor, and a short-circuit reflect. We performed both the multiline TRL calibration [19] and then used a series-resistor calibration to compute the capacitance per unit length of the CPWs (C_o) [20], which allowed us to transform the reference impedance to 50 Ω [21]. For frequencies from 100 MHz to 110 GHz, we used the multiline TRL calibration to correct the S-parameter data. Below, we used the series-resistor

calibration to correct the S-parameter data. These on-wafer calibrations allowed us to correct all subsequent S-parameters to the center of the thru and to 50 Ω.

Fortuitously, the multiline TRL calibration yielded the propagation constant of the CPW, which is written as $\gamma = \sqrt{(R + i\omega L)(i\omega C_o)}$ where ω is the angular frequency and R, L, and C_o are the distributed resistance, inductance, and capacitance per unit length of the CPW as a function of frequency. Recall that the conductance was assumed to be zero, following Ref. [21]. These results served as a check for the fitting algorithm, which we will discuss later.

VII. RESULTS

To test our algorithm, we corrected the six different CPW transmission lines lengths $\ell = (1.000, 1.735, 3.135, 4.595, 7.615, 9.970)$ mm to the center of the thru. We chose the same CPWs transmission line that were included in the calibration set. We then applied Eisenstadt and Eo [5] analytical model, (10)-(13), and our nonlinear least-squares algorithm, extracting R, L, C and G (orange lines, Fig. 3-6, respectively). Next, we applied our algorithm, allowing all four distributed circuit parameters vary (blue lines, Fig. 3-6, respectively). We repeated the same algorithm constraining the capacitance, C, and conductance, G, to match the result from multiline TRL (green lines, Fig. 3-6, respectively). This constraint demonstrates that one can further improve the nonlinear regression if some of the fit parameters are known. Finally, we compared these results to what we obtained from multiline TRL (black lines, Fig. 3-6, respectively). Although we computed R, L, C and G for each line, we only show the results for the longest line ($\ell = 9.970$ mm) for clarity. All the figures have the same legend, hence it is only show in Fig. 3.
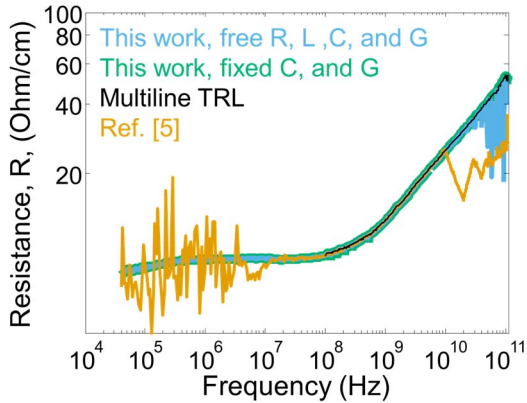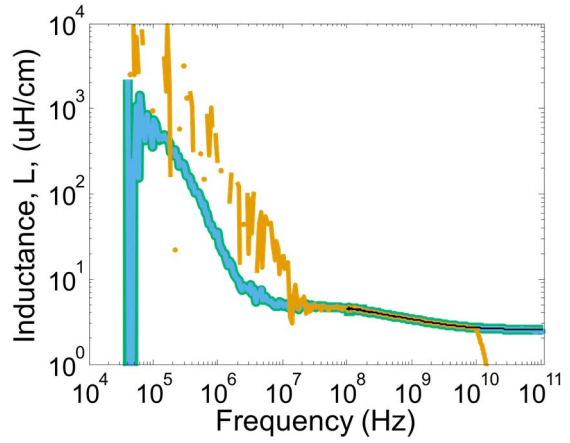

Fig. 3. Resistance per unit length comparison.

Fig. 4. Inductance per unit length comparison. The case where $R, L, C,$ and G are free is shown, however it overlaps with the blue line.
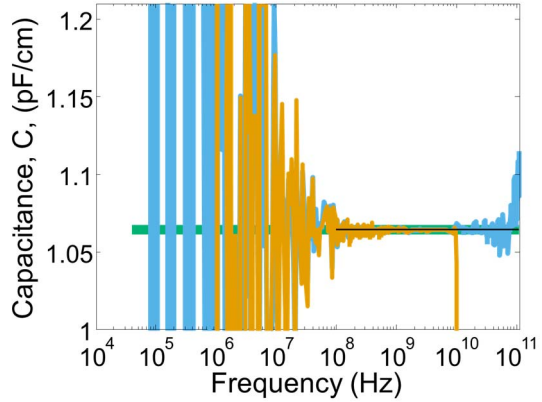

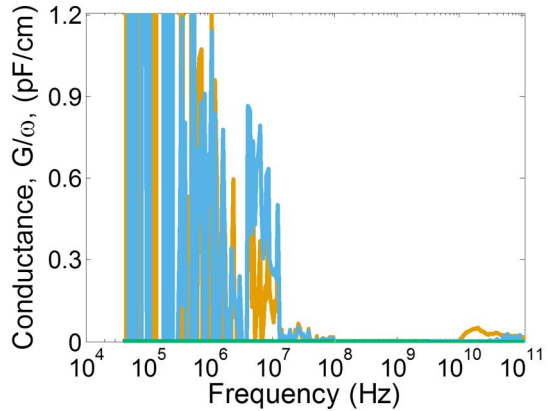Fig. 5. Capacitance per unit length comparison.

Fig. 6. Conductance per unit length comparison.

VIII. CONCLUSION

In this paper, we demonstrated an algorithm to extract the distributed circuit parameters from a nonlinear least-squares regression. It has long been established that analytical model fails at high frequencies due to branch cuts in the complex plane. Here, we showed that by scaling the distributed circuit

parameters we can accurately extract the distributed circuit parameters even at high frequencies where the analytical expression breaks down. This algorithm allowed us to increase the range of frequencies that we could extract the distributed circuit parameters to the bounds of our measurement.

We summarize by stating that the distributed circuit parameters of a corrected transmission line can be computed directly from a least-squares regression, so long as the circuit parameters are scaled according to the physics that controls their frequency dependence.

REFERENCES

[1] B. F. Ronalds, "Francis Ronalds (1788 #x2013;1873): The First Electrical Engineer? [Scanning Our Past]," *Proc. IEEE*, vol. 104, no. 7, pp. 1489–1498, Jul. 2016.

[2] O. Heaviside, "XXXIX. On the electromagnetic effects due to the motion of electrification through a dielectric," *Philos. Mag.*, vol. 27, no. 167, pp. 324–339, Apr. 1889.

[3] H. Klingbeil and W. Heinrich, "Calculation of CPW AC resistance and inductance using a quasi-static mode-matching approach," *IEEE Trans. Microw. Theory Tech.*, vol. 42, no. 6, pp. 1004–1007, Jun. 1994.

[4] S. Gevorgian, L. J. P. Linner, and E. L. Kollberg, "CAD models for shielded multilayered CPW," *IEEE Trans. Microw. Theory Tech.*, vol. 43, no. 4, pp. 772–779, Apr. 1995.

[5] W. R. Eisenstadt and Y. Eo, "S-parameter-based IC interconnect transmission line characterization," *IEEE Trans. Compon. Hybrids Manuf. Technol.*, vol. 15, no. 4, pp. 483–490, Aug. 1992.

[6] T. Coleman and Y. Li, "An Interior Trust Region Approach for Nonlinear Minimization Subject to Bounds," *SIAM J. Optim.*, vol. 6, no. 2, pp. 418–445, May 1996.

[7] K. Levenberg, "A method for the solution of certain non-linear problems in least squares," *Q. Appl. Math.*, vol. 2, no. 2, pp. 164–168, 1944.

[8] D. Marquardt, "An Algorithm for Least-Squares Estimation of Nonlinear Parameters," *J. Soc. Ind. Appl. Math.*, vol. 11, no. 2, pp. 431–441, Jun. 1963.

[9] D. A. Frickey, "Conversions between S, Z, Y, H, ABCD, and T parameters which are valid for complex source and load impedances," *IEEE Trans. Microw. Theory Tech.*, vol. 42, no. 2, pp. 205–211, Feb. 1994.

[10] N. D. Orloff, "Broadband In-plane Relative Permittivity Characterization of Ruddlesden-Popper Sr(n+1)Ti(n)O(3n+1) Thin Films," 2010.

[11] J. C. Booth, "Quantitiative Permittivity Measurements of Nanoliter Liquid Volumes in Microfluidic Channels to 40 GHz," *IEEE Trans. Instrum. Meas.*, vol. 59, no. 12, p. 3279 to 3288, 2010.

[12] C.-H. Lee *et al.*, "Exploiting dimensionality and defect mitigation to create tunable microwave dielectrics," *Nature*, vol. 502, no. 7472, pp. 532–536, Oct. 2013.

[13] F. Mirri *et al.*, "Lightweight, Flexible, High-Performance Carbon Nanotube Cables Made by Scalable Flow Coating," *ACS Appl. Mater. Interfaces*, vol. 8, no. 7, pp. 4903–4910, Feb. 2016.

[14] C. A. E. Little, N. D. Orloff, I. E. Hanemann, C. J. Long, V. M. Bright, and J. C. Booth, "Modeling electrical double-layer effects for microfluidic impedance spectroscopy from 100 kHz to 110 GHz," *Lab. Chip*, vol. 17, no. 15, pp. 2674–2681, Jul. 2017.

[15] D. M. Pozar, "Considerations for millimeter wave printed antennas," *IEEE Trans. Antennas Propag.*, vol. 31, no. 5, pp. 740–747, 1983.

[16] R. Materese, "A General Waveguide Circuit Theory," *NIST*, 01-Oct-1992. [Online]. Available: https://www.nist.gov/node/639581. [Accessed: 26-Nov-2016].

[17] B. Y. Hu, "Kramers–Kronig in two lines," *Am. J. Phys.*, vol. 57, no. 9, pp. 821–821, Sep. 1989.

[18] R. B. Marks, "Formulations of the Basic Vector Network Analyzer Error Model including Switch-Terms," in *50th ARFTG Conference Digest*, 1997, vol. 32, pp. 115–126.

[19] R. B. Marks, "A multiline method of network analyzer calibration," *IEEE Trans. Microw. Theory Tech.*, vol. 39, no. 7, pp. 1205–1215, Jul. 1991.

[20] D. F. Williams and D. K. Walker, "Series-Resistor Calibration," in *50th ARFTG Conference Digest*, 1997, vol. 32, pp. 131–137.

[21] N. D. Orloff *et al.*, "A Compact Variable-Temperature Broadband Series-Resistor Calibration," *IEEE Trans. Microw. Theory Tech.*, vol. 59, no. 1, pp. 188–195, Jan. 2011.